SAGE-Hindawi Access to Research
International Journal of Electrochemistry
Volume 2011, Article ID 968512, 6 pages
doi:10.4061/2011/968512

Research Article

Diffusivity of Point Defects in the Passive Film on Stainless Steel

A. Fattah-alhosseini, M. H. Alemi, and S. Banaei

Faculty of Engineering, Bu-Ali Sina University, Hamedan 65178-38695, Iran

Correspondence should be addressed to A. Fattah-alhosseini, a.fattah@basu.ac.ir

Received 25 October 2010; Revised 2 December 2010; Accepted 14 December 2010

Academic Editor: Sergio Ferro

The semiconductor properties of passive films formed on AISI 316 stainless steel in sulfuric acid solution were studied by employing Mott-Schottky analysis in conjunction with the point defect model. The donor density of the passive films, which can be estimated by the Mott-Schottky plots, changes depending on the film formation potentials. Based on the Mott-Schottky analysis, an exponential relationship between donor density and the film formation potentials of the passive films was developed. The results showed that the donor densities evaluated from Mott-Schottky plots are in the range 2-3 $\times 10^{21}$ cm^{-3} and decreased with the film formation potential. By assuming that the donors are oxygen ion vacancies and/or cation interstitials, the diffusion coefficient of the donors, (D_O), is calculated to be approximately 3.12×10^{-16} cm^2/s.

1. Introduction

Compared with many theories qualitatively describing the passive state, the point defect model (PDM) provides a microscopic description of the growth and breakdown of a passive film and an analytical expression for the flux and the concentration of vacancies within the passive film, which affords an opportunity for quantitative analysis [1–3]. The PDM is based on the migration of point defects (oxygen and metal vacancies) under the influence of the electrostatic field in the passive film. Because the passive film is grown into the metal by the generation of oxygen vacancies at the metal/passive film interface and by their annihilation at the passive film/solution interface, the transport properties and spatial distribution of oxygen vacancies or metal cations within the passive film are of great interest [4]. A key parameter in describing the transport of point defects and hence the kinetics of passive film growth is the diffusivity of the point defects (D_O) . By using Mott-Schottky analysis in conjunction with the PDM for passive films, Sikora et al. [5] determined the oxygen vacancy diffusion coefficient in the WO_{3-x} passive film formed on tungsten in phosphoric acid (pH 0.96) solution at ambient temperature to be in the range of 10^{-14}-10^{-15} cm^{2}s^{-1}. Although it is impossible to distinguish between oxygen vacancy and cation interstitial conducting passive films on the basis of PDM itself, the assumption is still valid in this case due to the fact that WO_3 is known as priori to be oxygen vacancy. Also, by this method the diffusion coefficient of the donors in the passive film formed on AISI 316L stainless steel is determined [6].

It is well recognized that passive films exhibit semiconductor properties, and numerous attempts have been made to interpret these properties in terms of classical theories for lowly and moderately doped semiconductors. However, direct measurement of passive film composition (e.g., by determining the O : M ratio through the film) and indirect electrochemical studies (e.g., by Mott-Schottky analysis) have shown that the vacancy concentrations may be very large (of the order of 10^{19}–10^{21}cm^{-3}) [7].

However, there is still lack of study on the diffusivities of point defects in the passive film formed on stainless steel, which is the most extensively used engineering material in industries. In this work, the Mott-Schottky analysis of AISI 316 stainless steel (316) in sulfuric acid solution was performed, and the defects concentration was measured as a function of the film formation potential (E). The relationship between the donor density (N_D) and the film formation potential is discussed in order to understand the property of the passivation of stainless steel.

Table 1: Nominal chemical composition of 316.

Elements	Cr	Ni	Mo	Mn	Si	C	P	S	Fe
316/wt%	16.5	12.5	2.22	1.42	0.42	0.09	0.04	0.005	Bal

2. Materials and Methods

Specimens were cut from 1-cm-diameter rods of 316; the nominal composition is given in the Table 1. The samples were placed in stainless steel sacks and were annealed in inert environment (Ar gas) to eliminate the cold work effect due to cutting process. The annealing was performed at 1050°C for 90 min followed by water quenching. A mechanically polished 316 sample was used as a reference point (polishing under water with SiC paper up to 1200 grit size). Prior to each experiment, samples were degreased in an ultrasonic acetone/ethanol mixed bath, rinsed with distilled water, and finally dried.

All electrochemical measurements were performed in a conventional three-electrode cell. The counter electrode was a Pt plate, and all potentials were measured against a saturated calomel electrode (SCE) connected to the cell via a Luggin probe. All experiments were performed at ambient temperature (23–25°C) in 0.05 M H_2SO_4, pH 1.5.

The polarization curve was obtained using a PARSTAT 2273 advanced electrochemical system with 1 mV/s scan rate. The capacitance of the interface was also recorded with a PARSTAT 2273 advanced electrochemical system. Prior to capacitance measurement, working electrodes were initially reduced potentiostatically at −1.2 V for 5 min and then polarized at a desired formation potential for 1 h to form a steady oxide film. Capacitance measurements were carried out on the anodic films at a frequency of 1 kHz using a 10 mV AC signal and a step rate of 25 mV, in the cathodic direction. An important point to be considered in the Mott-Schottky analysis is that the measured capacitance value is influenced by frequency. In order to obtain an optimized frequency for capacitance measurements, a curve of capacitance as a function of frequency at stable potential was obtained. 1 kHz was chosen because a stable capacitance value was obtained as the frequency varied from 1 to 0.001 kHz. The measurement of the capacitance-potential profile of the passive film formed at different potentials was carried out on different samples.

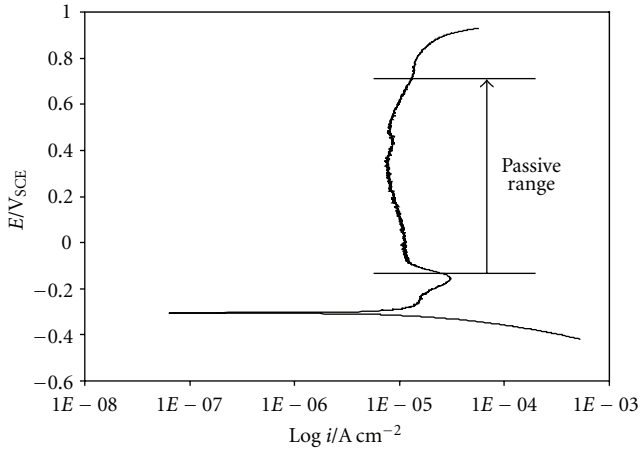

Figure 1: Potentiodynamic polarization curve of 316 in 0.05 M H_2SO_4 solution with 1 mV/s scan rate.

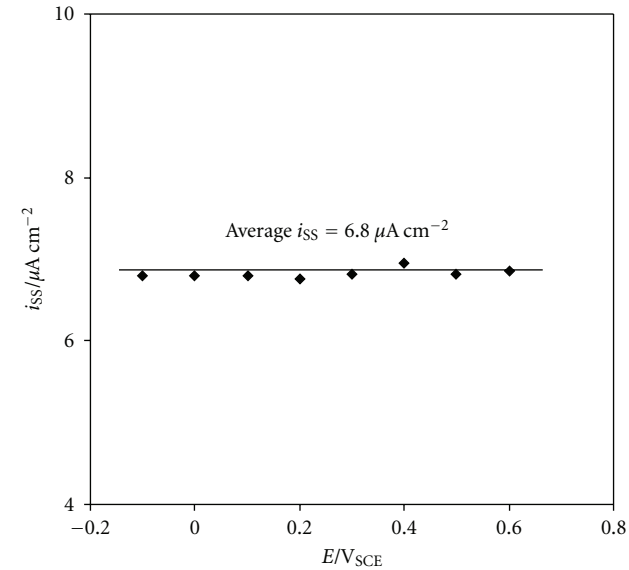

Figure 2: Steady-state current density obtained during the potentiostatic growth of the passive films at different film formation potentials for 1 h.

3. Results and Discussion

3.1. Polarization Behavior. Figure 1 shows the potentiodynamic curve for 316 electrode in 0.05 M H_2SO_4. From the polarization curve, the passive range was determined to be from about −0.2 to 0.6 V_{SCE}. It was observed that before the electrode was transferred to a passive state, an active current peak occurred at around −0.15 V_{SCE}, which could be attributed to the oxidation of Fe^{2+} to Fe^{3+}ions in the passive film [6].

Films were grown at each potential for 1 h to insure that the system was in steady state. During the formation of the oxide films on working electrode, the current density was monitored. It was observed that the current density diminishes with time until a constant value is reached and a steady-state established. Figure 2 shows the values of the steady state passive current density (i_{SS}) versus the film formation potential. The steady-state current density is approximately 6.8 μA cm^{-2}.

3.2. Mott-Schottky Measurements. The capacitance of the passive film (C_T) is considered to be the combination of

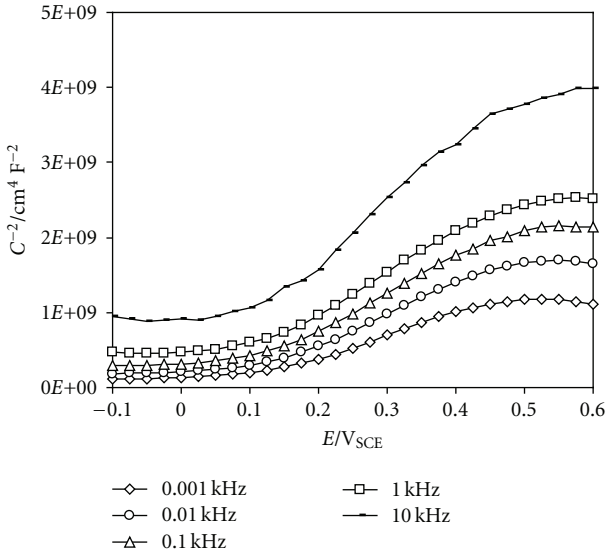

Figure 3: Mott-Schottky plots at different frequencies of the passive films formed on surface in 0.05 M H_2SO_4. The electrode is passivated for 1 h at 0.6 V_{SCE}.

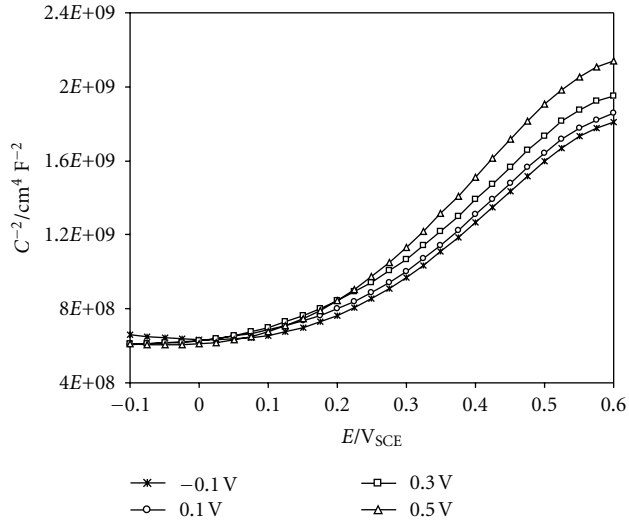

Figure 4: Mott-Schottky curves for passive films formed on 316 at different film formation potentials for 1 h in 0.05 M H_2SO_4.

two series capacitances: the space charge capacitance (C_{SC}) at the film/solution interface and the classical Helmholtz capacitance (C_H) [8]:

$$\frac{1}{C_T} = \frac{1}{C_{SC}} + \frac{1}{C_H}. \tag{1}$$

Assuming that the Helmholtz capacitance is much larger than the space charge capacitance, the measured C_T is equal to C_{SC}. Therefore, the data points in C_{sc}^{-2} versus E plots can describe the semiconducting behavior of the passive film. Given a correct value of C_{SC} capacitance, the electronic properties are usually deduced from the Mott-Schottky relation [8, 9] as follows:

$$\frac{1}{C_T^2} = \frac{1}{C_{SC}^2} = \frac{2}{\varepsilon\varepsilon_0 q N_q}\left(E - E_{fb} - \frac{k_B T}{q}\right), \tag{2}$$

where q is the elementary charge (-1.602×10^{-19} C for an electron and $+1.602 \times 10^{-19}$ C for electron hole), N_q is the density of charge carriers (N_A for acceptors and N_D for donors), (ε is the dielectric constant of the passive film, which is assumed as 15.6 [10]), ε_0 is the vacuum permittivity (8.854×10^{-14} F/cm), k_B is the Boltzmann constant (1.38×10^{-23} J/K), T is the absolute temperature, E is the applied potential, and E_{fb} is the flat-band potential. At room temperature, k_BT/q is neglected because it is only about 25 mV. For a p-type semiconductor, C_{sc}^{-2} versus E should be linear with a negative slope that is inversely proportional to the acceptor density. On the other hand, an n-type semiconductor yields a positive slope which is inversely proportional to the donor density.

Figure 3 shows the Mott-Schottky plots obtained at different frequencies for a passive film formed on surface of 316 in 0.05 M H_2SO_4. As was expected, the Mott-Schottky plots are frequency dependent. However, one can note that below 1 kHz the experimental data are quite stable. Yet, this allowed us to set a threshold frequency in the experimental protocol before conducting any experiments on the surface. According to (2), the slope of the linear portion of C_{sc}^{-2} versus E plot, gives the charge carrier density (N_q) from the following equation:

$$N_q = \frac{2}{q \cdot \varepsilon \cdot \varepsilon_0 \cdot s}, \tag{3}$$

where s is the slope of the Mott-Schottky plot in the linear-region of interest. A higher frequency was selected to minimize the contribution of Helmholtz capacitance, which results from charge redistributions within the solution at the surface. Helmholtz capacitance neither affects the C_{sc}^{-2} versus E plot, nor the calculation of charge carrier density within the passive film, as only the linear region of the graph is considered to calculate the slope [10].

The Mott-Schottky plots for the passive films formed at different film formation potentials on 316 are shown in Figure 4. The film formation potential varies between −0.1 and 0.6 V_{SCE}. Four typical examples of Mott-Schottky plots measured at different film formation potentials are shown in Figure 4. From this figure, a linear part can be easily distinguished for potentials greater than 0.0 V_{SCE}. The decrease of capacitance with the applied potential in Figure 4 is attributed to an increase in the thickness of the electron-depleted layer and a diminishing number of charge carriers (donor for an n-type semiconductor), that is the region close to the film/solution is depleted in electrons.

The slopes of the Mott-Schottky curve of the passive film formed at various formation potentials were different. At a formation potential lower than 0.6 V_{SCE}, the value of the Mott-Schottky curve slopes increased with the increase of the formation potential. Therefore, in the following analysis, the potential range from −0.1 to 0.5 V_{SCE} for 316 was chosen to explain the relationship between donor density and formation potential.

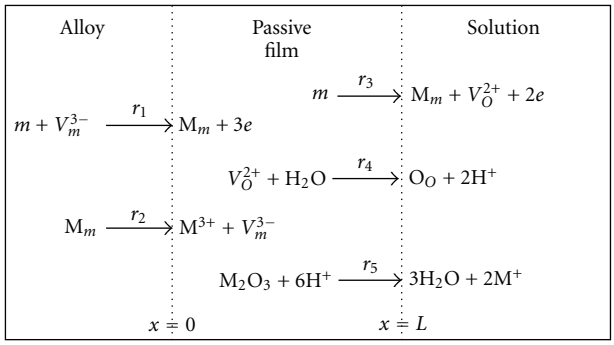

Figure 5: Schematic representation of five electrochemical processes which occur within the passive film according to the PDM.

The observed values of N_D obtained for 316 are in the range of 2-3 $\times$ 10^{21} cm^{-3}, which is comparable, and in the similar range reported for the passive film of stainless steels. Di Paola reported a donor density of 3.8×10^{21} cm^{-3} for 304 passivated in 0.5 kmol/m^3 H_2SO_4 at 0.2 V_{SCE}, which agrees with the present data [11]. The density of charge carriers has been observed to be a strong function of the passive film formation potential. The donor density of passive film of 316L was observed to decrease with an increase in the formation potential.

In general, the changes in N_D do not correspond to impurity concentration but rather to the nonstoichiometry defects in the space charge region or due to the disordered character of the passive film. The donors in semiconducting passive layers are defects themselves, including oxygen ion vacancies and/or cation interstitials. These defects act as dopants, that is, oxygen ion vacancies and/or cation interstitials imparting n-type character. Both oxygen ion vacancies and cation interstitials are electron donors. The presence of such dopant prevents migration of cations from alloys and penetration of harmful anions, such as SO_4^{2-}, from the solution, thereby improving the corrosion resistance. The decrease in N_D means impoverishment of these species, which neutralizes the dopant. Higher N_D values are strong indication of a nonstoichiometric or highly disordered passive film [12].

4. Relationship between N_D and E

A number of models have been proposed to explain the kinetic, thermodynamic, structural, and electronic properties of passive film formation. Among all the models, PDM is widely accepted. PDM provides microscopic description of the growth and breakdown of the passive film under steady-state and transient conditions. This model is based on the migration of the point defects under the influence of the electrostatic field in the passive film. A passive film is envisaged to grow into the alloy by generation of the oxygen ion vacancies at the alloy/passive film interface and by their annihilation at the passive film/solution interface. Figure 5 shows the dynamic and steady-state properties of a passive film expressed by five electrochemical reactions basing on the PDM [13].

(1) Metal vacancies are annihilated and produced at the alloy/passive film interface:

$$m + V_m^{3-} \xrightarrow{r_1} M_m + 3e, \qquad M_m \xrightarrow{r_2} M^{3+} + V_m^{3-}. \tag{4}$$

(2) Oxygen ion vacancies are produced and annihilated at the passive film/solution interface:

$$m \xrightarrow{r_3} M_m + V_O^{2+} + 2e, \tag{5}$$

$$V_O^{2+} + H_2O \xrightarrow{r_4} O_O + 2H^+. \tag{6}$$

(3) The film dissolves chemically at the passive film/solution interface:

$$M_2O_3 + 6H^+ \xrightarrow{r_5} 3H_2O + 2M^{3+}. \tag{7}$$

m represents metal atom, M_m metal cations in film, O_O oxygen anions in film, V_m^{3-} metal vacancy, V_O^{2+} oxygen ion vacancy, M^{3+} metal ion in solution, and M_2O_3 chemical expression of the passive film.

Because the passive films show n-type semiconductive behavior, the donor density (oxygen ion vacancy) is much larger than that of the acceptor (metal vacancy). Reactions (5) and (6) are dominant in the model. The flux of oxygen ion vacancy during the passive film can be expressed by Nernst-Planck equation [13, 14]:

$$J_O = -D_O \frac{\partial C_O}{\partial x} + 2KD_O C_O, \tag{8}$$

where D_O is the diffusion coefficient of oxygen ion vacancy, $K = k_e F/RT$, and k_e is the electric field strength of the passive film. The oxygen ion vacancy density in the passive film was obtained by solving the following equation:

$$C_O(x) = \left(C_O(L) - \frac{J_O}{2KD_O}\right) \exp(-2KL) \exp(2Kx) + \frac{J_O}{2KD_O}, \tag{9}$$

where L is the thickness of the passive film. The lower concentration of oxygen ion vacancy close to the passive film/solution interface results in the occurrence of an insulating layer. The almost constant concentration of oxygen ion vacancy close to the alloy/passive film interface should result in a linear Mott-Schottky plot. Accordingly, the donor density calculated from Mott-Schottky curves was the oxygen ion vacancy concentration at the alloy/passive film interface [13, 14].

$$N_D = C_O(0) = \left(C_O(L) - \frac{J_O}{2KD_O}\right) \exp(-2KL) + \frac{J_O}{2kD_O},$$

$$N_D = C_O(L) \exp(-2KL) + \frac{J_O}{2KD_O}(1 - \exp(-2KL)). \tag{10}$$

As reaction (6) is dominant, J_O equals the rate of production of oxygen ion vacancy at the passive film/solution interface. Accordingly,

$$\begin{aligned} J_O &= r_4 C_O(L), \\ r_4 &= r_4^0 \exp\left(2\alpha_4 \gamma \phi_{f/s}\right), \\ \phi_{f/s} &= \phi_{f/s}^0 + \alpha E + \beta \mathrm{pH}, \end{aligned} \tag{11}$$

where r_4 is the rate constant for reaction (6). The rate constant depends on the potential drop across the passive film/solution interface, $\phi_{f/s}$. r_4^0 is the rate constant for $\phi_{f/s}^0 = 0$, α_4 is the transfer coefficient, $\gamma = F/RT$, $\phi_{f/s}^0$ is the potential drop at the passive film/solution interface when $E = 0$, pH = 0, and α, β are constant parameters.

$$\begin{aligned} C_O(L) &= \frac{J_O}{r_4} = \frac{J_O}{r_4^0 \exp\left(2\alpha_4 \gamma \phi_{f/s}\right)} \\ &= \frac{J_O}{r_4^0 \exp\left(2\alpha_4 \gamma \left(\phi_{f/s}^0 + \alpha E + \beta \mathrm{pH}\right)\right)}, \\ N_D &= \frac{J_O}{r_4^0 \exp\left(2\alpha_4 \gamma \left(\phi_{f/s}^0 + \alpha E + \beta \mathrm{pH}\right)\right)} \exp(-2KL) \\ &\quad + \frac{J_O}{2KD_O}(1 - \exp(-2KL)), \\ N_D &= \frac{J_O}{r_4^0} \exp\left(-2\alpha_4 \gamma \left(\phi_{f/s}^0 + \alpha E + \beta \mathrm{pH}\right)\right) \exp(-2KL) \\ &\quad + \frac{J_O}{2KD_O}(1 - \exp(-2KL)), \\ KL &= (k_e \gamma)L = \left(k_e \frac{F}{RT}\right)L = \left(\frac{k_e F}{RT}\right)L = \frac{FE}{RT}, \\ N_D &= \frac{J_O}{r_4^0} \exp\left(-2\alpha_4 \gamma \left(\phi_{f/s}^0 + \alpha E + \beta \mathrm{pH}\right)\right) \exp\left(\frac{-2FE}{RT}\right) \\ &\quad + \frac{J_O}{2KD_O}\left(1 - \exp\left(\frac{-2FE}{RT}\right)\right). \end{aligned} \tag{12}$$

Since for thin passive films (<10 nm thick), E may be as large as 10^6-10^7 V/cm [14], the value of FE is much larger than RT. So,

$$\begin{aligned} 1 - \exp\left(\frac{-2FE}{RT}\right) &\longrightarrow 1, \\ \omega_1 &= \frac{J_O}{r_4^0} \exp\left(-2\alpha_4 \gamma \left(\phi_{f/s}^0 + \beta \mathrm{pH}\right)\right), \\ b &= \left(\frac{-2F}{RT} - 2\alpha_4 \gamma \alpha\right) < 0, \\ \omega_2 &= \frac{J_O}{2KD_O}. \end{aligned} \tag{13}$$

Therefore,

$$N_D = \omega_1 \exp(bE) + \omega_2. \tag{14}$$

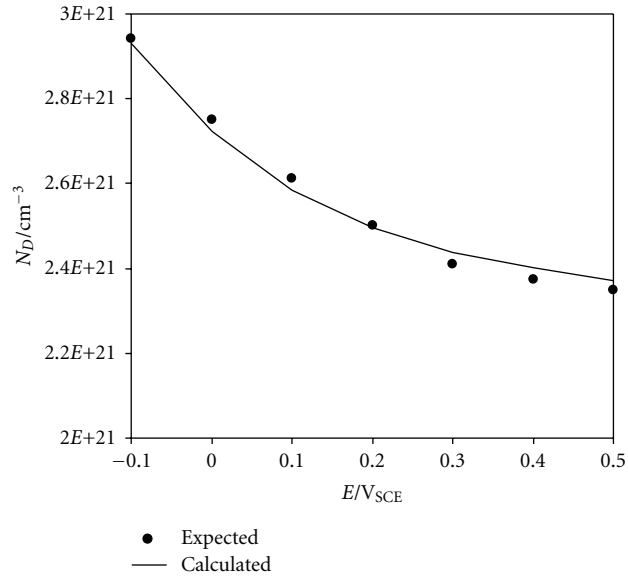

Figure 6: Curve of donor density as function of film formation potential of the passive films formed on 316 in 0.05 M H_2SO_4.

So, the donor density of the passive film should decrease exponentially with the increase of the formation potential [15]. The donor density has been calculated from capacitance measurements for films formed at different formation potentials. The best exponential fit to the experimental data is shown in Figure 6. The data plotted in Figure 6 show that the donor density decreases with increasing the film formation potential, which is in agreement with the prediction of PDM.

Sikora and Macdonald have shown that the relationship between N_D and the film formation potential can be developed theoretically on the basis of the PDM, assuming that the defects are the electron donor. This theoretical relationship yields a good fit to the experimental results and allows the diffusivity of the defects in the passive film to be calculated. The relevant equation describing the dependence of the donor density on the film formation potential is shown as (14), where ω_1, ω_2, and b are unknown constants that are to be determined from the experimental data [5]. Based on the nonlinear fitting of the experimental data by software, the exponential relationship between the donor density (N_D) and the film formation potential (E) is derived as

$$N_D = 0.392 \times 10^{21} \exp(-4.37E) + 2.332 \times 10^{21}. \tag{15}$$

According to the PDM, the flux of oxygen ion vacancy through the passive film is essential to the film growth process, which supports the existence of oxygen ion vacancy in the film regardless of its concentration. In this concept, the dominant point defects in the passive film are considered to be oxygen ion vacancies and/or cation interstitials acting as electron donors. However, as it is not possible to separate the contribution of oxygen ion vacancies and cation interstitials on the measured diffusivity value based on the PDM, the diffusivity is considered that for the combination of these two

point defects [16]. The diffusion coefficient can be calculated from (15) by [6]:

$$D_O = \frac{J_O}{2K\omega_2} = \frac{J_O RT}{2F\omega_2 k_e}, \quad (16)$$

$$J_O = -\frac{i_{SS}}{2e}. \quad (17)$$

k_e was determined to be approximately 1.02×10^6 V/cm by Szklarska-Smialowska and Kozlowski [16] for the passive film grown on iron. Therefore, it is assumed that the value of k_e for the passive film on stainless steel to be approximately 10^6 V/cm. Substitution of k_e ($\approx 10^6$ V/cm), i_{SS} ($\approx 6.8 \times 10^{-6}$ A cm^{-2}), e (-1.602×10^{-19} C), ω_2 (2.332×10^{21} cm^{-3}), R (8.314 J/mol K), T (298 K), and F (96500 C mol/e) into (16) and (17) yields $D_O = 1.17 \times 10^{-16}$ cm^2/s. Taking into account the error caused by the assumption of k_e in (16), the diffusion coefficient of defects in the passive film formed on 316 in 0.05 M H_2SO_4 solution is estimated to be approximately in the range of 10^{-16} cm^2/s.

5. Summary

Potentiodynamic polarization studies demonstrate that 316 displays a wide passive range in 0.05 M H_2SO_4 at ambient temperature. Potentiostatic polarization tests revealed that the steady-state current density (i_{SS}) through the passive film formed on 316 for 1 h was independent of formation potential, which is well consistent with the postulation of the PDM. Based on the Mott-Schottky analysis, it was shown that the calculated donor density decreases exponentially with increasing formation potential. The experimental data were interpreted in terms of the PDM for the passivity of 0.05 M H_2SO_4, assuming that the donors are defects including oxygen vacancies and cation interstitials. The diffusivity of donors in the passive film on 316 was calculated to be approximately in the range of 10^{-16} cm^2/s.

References

[1] D. D. Macdonald, "On the tenuous nature of passivity and its role in the isolation of HLNW," *Journal of Nuclear Materials*, vol. 379, no. 1–3, pp. 24–32, 2008.

[2] D. D. MacDonald, "On the existence of our metals-based civilization I. Phase-space analysis," *Journal of the Electrochemical Society*, vol. 153, no. 7, pp. B213–B224, 2006.

[3] D. D. Macdonald, "Point defect model for the passive state," *Journal of the Electrochemical Society*, vol. 139, no. 12, pp. 3434–3449, 1992.

[4] A. Fattah-alhosseini, A. Saatchi, M. A. Golozar, and K. Raeissi, "The transpassive dissolution mechanism of 316L stainless steel," *Electrochimica Acta*, vol. 54, no. 13, pp. 3645–3650, 2009.

[5] E. Sikora, J. Sikora, and D. D. Macdonald, "A new method for estimating the diffusivities of vacancies in passive films," *Electrochimica Acta*, vol. 41, no. 6, pp. 783–789, 1996.

[6] A. Fattah-Alhosseini, A. Saatchi, M. A. Golozar, and K. Raeissi, "The passivity of AISI 316L stainless steel in 0.05 M H_2SO_4," *Journal of Applied Electrochemistry*, vol. 40, no. 2, pp. 457–461, 2010.

[7] J. Sikora, E. Sikora, and D. D. MacDonald, "Electronic structure of the passive film on tungsten," *Electrochimica Acta*, vol. 45, no. 12, pp. 1875–1883, 2000.

[8] E. M. A. Martini and I. L. Muller, "Characterization of the film formed on iron borate solution by electrochemical impedance spectroscopy," *Corrosion Science*, vol. 42, no. 3, pp. 443–454, 2000.

[9] M. F. Montemor, M. G. S. Ferreira, N. E. Hakiki, and M. Da Cunha Belo, "Chemical composition and electronic structure of the oxide films formed on 316L stainless steel and nickel based alloys in high temperature aqueous environments," *Corrosion Science*, vol. 42, no. 9, pp. 1635–1650, 2000.

[10] K. S. Raja and D. A. Jones, "Effects of dissolved oxygen on passive behavior of stainless alloys," *Corrosion Science*, vol. 48, no. 7, pp. 1623–1638, 2006.

[11] A. D. Paola, "Semiconducting properties of passive films on stainless steels," *Electrochimica Acta*, vol. 34, no. 2, pp. 203–210, 1989.

[12] G. Goodlet, S. Faty, S. Cardoso et al., "The electronic properties of sputtered chromium and iron oxide films," *Corrosion Science*, vol. 46, no. 6, pp. 1479–1499, 2004.

[13] M. Vankeerberghen, "1D steady-state finite-element modelling of a bi-carrier one-layer oxide film," *Corrosion Science*, vol. 48, no. 11, pp. 3609–3628, 2006.

[14] B. Krishnamurthy, R. E. White, and H. J. Ploehn, "Electric field strength effects on time-dependent passivation of metal surfaces," *Electrochimica Acta*, vol. 47, no. 15, pp. 2505–2513, 2002.

[15] T. L. Sudesh, L. Wijesinghe, and D. J. Blackwood, "Photocurrent and capacitance investigations into the nature of the passive films on austenitic stainless steels," *Corrosion Science*, vol. 50, no. 1, pp. 23–34, 2008.

[16] Z. Szklarska-Smialowska and W. Kozlowski, in *Passivity of Metals and Semiconductors*, M. Froment, Ed., chapter 4, Elsevier, Amsterdam, The Netherlands, 1983.